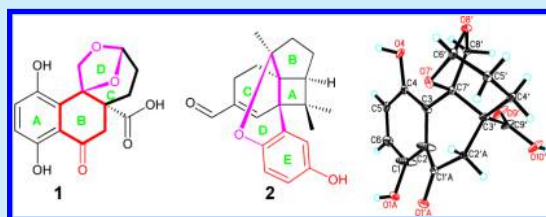


Cochlearols A and B, Polycyclic Meroterpenoids from the Fungus *Ganoderma cochlear* That Have Renoprotective ActivitiesMan Dou,^{†,§,¶} Lei Di,^{†,¶} Li-Li Zhou,^{‡,¶} Yong-Ming Yan,^{†,||} Xin-Long Wang,[†] Feng-Jiao Zhou,[†] Zhu-Liang Yang,[⊥] Rong-Tao Li,^{*,§} Fan-Fan Hou,^{*,‡} and Yong-Xian Cheng^{*,†}[†]State Key Laboratory of Phytochemistry and Plant Resources in West China, Kunming Institute of Botany, Chinese Academy of Sciences, 132 Lanhei Road, Kunming 650201, P. R. China[‡]State Key Laboratory of Organ Failure Research, Division of Nephrology, Nanfang Hospital, Southern Medical University, Guangzhou 510515, P. R. China[§]Faculty of Life Science and Technology, Kunming University of Science of Technology, Kunming 650500, P. R. China^{||}University of Chinese Academy of Sciences, Yuquan Road 19, Beijing 100049, P. R. China[⊥]Key Laboratory for Plant Diversity and Biogeography of East Asia, Kunming Institute of Botany, Chinese Academy of Sciences, Kunming 650201, P. R. China

S Supporting Information

ABSTRACT: (+)- and (−)-cochlearols A (1) and B (2), two meroterpenoids with novel polycyclic skeletons, were isolated from the fruiting bodies of the fungus *Ganoderma cochlear*. Their structures and stereochemistry were determined by using spectroscopic, computational and single-crystal X-ray diffraction methods. Cochlearol A is a new normeroterpenoid containing a naturally unusual dioxaspiro[4.5]decane motif. Biological studies showed that (−)-2 is a strong inhibitor of p-Smads, exhibiting renoprotective activities in TGF- β 1 induced rat renal proximal tubular cells.



The *Ganoderma* species are found throughout the world, especially in subtropical and tropical regions.¹ Several *Ganoderma* species are considered as Lingzhi in China and have been long known for their value in traditional Chinese medicine.² Although only *G. lucidum* and *G. sinense* are registered in the Pharmacopoeia of P. R. China and American Herbal Pharmacopoeia and Therapeutic Compendium, many other species are commonly used as Chinese folk medicines.

The medicinal importance of the *Ganoderma* species in the prevention and treatment of various diseases, such as cancer, hypertension, chronic bronchitis, and asthma, have stimulated growing interest. So far, triterpenoids, polysaccharides, alkaloids, sterols, lectins, peptides, and proteins have been isolated from this genus.^{3,4} Recently, we isolated a novel meroterpenoid with a 5/5/6/6 ring system from *Ganoderma lucidum* and showed it to be a p-Smad3 inhibitor.⁵

G. cochlear is medicinally consumed in China. Earlier and more recent reports reveal that this fungus contains triterpenoids and phenolic meroterpenoids.^{6–9} In our continuing efforts aimed at the isolation of natural products that are active against chronic kidney disease, we investigated *G. cochlear*. This effort resulted in the isolation of two novel meroterpenoids possessing respective 5/6/6/6 or 4/5/6/6/6 polycyclic ring systems.

Cochlearol A (1),¹⁰ obtained as yellow crystals (see the Supporting Information), has the molecular formula C₁₅H₁₄O₇ (9 degrees of unsaturation) derived from analysis of its HREIMS, ¹³C NMR, and DEPT spectra. The ¹³C NMR and DEPT spectra

show that this substance contains 15 carbons including four methylenes (one oxygenated), three methines [two olefinic, one hemiacetal at δ_{H} 5.54 (brs, H-6'), eight quaternary carbons (one ketone, one carbonyl, four olefinic (two of which are oxygenated), and two aliphatic carbons (one of which is oxygenated)]. The ¹H NMR spectrum (Table S1, Supporting Information) of 1 contains resonances at δ_{H} 7.06 (d, $J = 9.0$ Hz, H-5) and 6.82 (d, $J = 9.0$ Hz, H-6), which indicate the presence of a 1,2,3,4-tetrasubstituted benzene ring. The chemical shifts of C-1 (δ_{C} 157.5) and C-4 (δ_{C} 149.4) of the arene ring show that they are bonded to oxygens. Finally, the ¹H–¹H COSY spectrum of this substance exhibits correlations between H-5/H-6, H-4'/H-5'/H-6' (δ_{H} 5.54) (Figure 1).

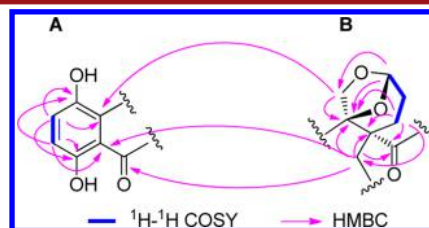
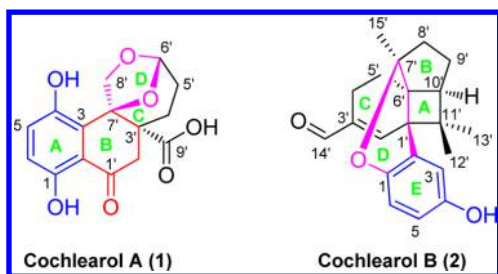


Figure 1. Key COSY and HMBC correlations of 1.

Received: September 23, 2014

Published: November 17, 2014



The structural architecture of **1** was determined mainly with the aid of HMBC correlations (Figure 1). Specifically, observed HMBC correlations between H-5/C-1, C-3, C-4, H-6/C-1, C-2, C-4, and H-2'/C-2, C-1' support the existence of a dihydroxy-substituted phenone fragment (A in Figure 1) in **1**, while correlations between H-6'/C-7', C-8', H-4'/C-2', C-3', C-7', C-9', and H-2'/C-3', C-4', C-7', C-9' strongly suggest the presence of the carboxy-substituted bicyclic acetal fragment (B). The conclusion that the structure of **1** is comprised of fragments A and B linked via C-3–C-7' and C-1'–C-2' is supported by the observed HMBC correlations between H-8'/C-3 and H-2'/C-1'. In addition, the TLC tailing behavior of **1** along with its molecular formula indicates that it contains a carboxylic acid group.

The relative configurations of the three stereogenic centers in **1** were assigned by analysis of the ROESY spectrum. Specifically, the correlations between H-8'b/H-4'a, H-2'a/H-4'b, and H-2'a/H-5'a show that the B-ring COOH and CH₂-8' methylene moieties are *cis*. This conclusion is confirmed by carrying out X-ray diffraction analysis of single crystals (cyclohexane/acetone, 1:1) (Figure 2).¹¹

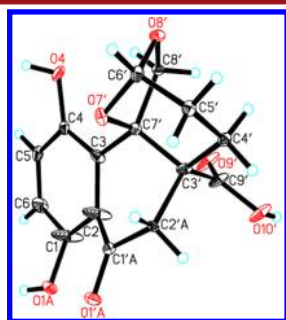


Figure 2. Plot of the X-ray crystallographic data of (\pm)-**1**.

The optical rotation and X-ray diffraction data both indicate that **1** was isolated as a racemic mixture. Subsequent chiral separation by HPLC afforded (+)-**1** and (–)-**1**, whose absolute configurations were assigned as 3'S,6'R,7'S for (+)-**1** and 3'R,6'S,7'R for (–)-**1**, respectively, by utilizing computational methods (Supporting Information). Notably, apart from a 1,4-dihydroxybenzene moiety and a missing carbon linked to C-7', the partial structure of **1** is that of a monoterpene. However, the separation between C-6'–C-7' and the presence of C-3–C-7' bond and an unusual 1,3-dioxolane suggest that **1** is a new meroterpenoid with a unique 5/6/6/6 ring system and a naturally unusual dioxaspiro[4.5]decane motif.

Cochlearol B (**2**),¹² obtained as a yellow amorphous powder, has the molecular formula C₂₁H₂₄O₃ (10 degrees of unsaturation) as deduced from its HREIMS, ¹³C NMR, and DEPT spectra. The ¹³C NMR and DEPT spectra show that this substance contains 21 carbons, including three methyls, four methylenes, six methines (one aldehyde, δ_H 9.55 (s, H-14), four

olefinic and one aliphatic), and eight quaternary carbons (four olefinic including two oxygenated and four aliphatic). The ¹H NMR spectrum of **2** contains resonances for a typical ABX spin system (δ_H 6.80, d, *J* = 2.2 Hz, H-3; δ_H 6.65, dd, *J* = 8.5, 2.2 Hz, H-5; δ_H 6.68, d, *J* = 8.5 Hz, H-6). Apart from those associated with a substituted benzene moiety, the remaining signals appear to be associated with protons in a terpenoid derivative.

The structure of **2** was elucidated using 2D NMR experiments. The presence of ¹H–¹H COSY correlations between H-8'/H-9'/H-10' along with HMBC correlations between H-8'/C-7', C-10', C-15'; H-15'/C-6', C-7'; H-9'/C-6', C-11'; H-10'/C-1', C-6', C-7', C-11', C-13' indicate that two isoprenyl moieties are present in fragment (A, Figure 3) of **2**. The structural fragment B

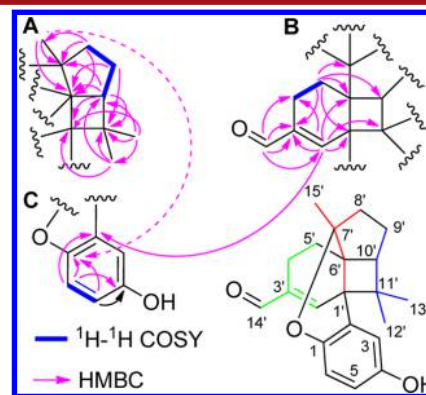


Figure 3. Key COSY and HMBC correlations of **2**; blue, red, and green in **2** represent three independent isoprenyl moieties.

is revealed by a ¹H–¹H COSY correlation between H-4'/H-5'. In addition, the presence of an isoprenyl related moiety in fragment B is supported by the HMBC correlations between H-14'/C-2', C-3', C-4', H-2'/C-3', C-4', H-5'/C-3'. The bonding pattern connecting fragments A and B in **2** is deduced by the observed HMBC correlations between H-5'/C-6', C-7', C-10', H-2'/C-1', C-6', C-11'.

Following completion of this structural elucidation, a literature search revealed that the terpenoid part of **2** is actually identical to italicen-15-al, a natural product previously isolated from *Lantana* oil.¹³ HMBC correlations between H-5/C-1, C-4, H-6/C-1, C-2 C-4 show that, like that of **1**, the structure of **2** contains a 1,4-dihydroxybenzene moiety (fragment C) that is connected to fragment A via C-2–C-1' and C-1–O–C-7'. This conclusion is supported by the HMBC correlations observed between H-2'/C-2 and a weak correlation between H-15'/C-1. Thus, the planar structure of cochlearol B is **2**. The correlations between H-2'/H-13', H-3/H-12', H-10'/H-13', H-5'/H-15', and H-12'/H-9' seen in the ROESY spectrum support the assignment of the relative configurations of the stereogenic centers in **2** that are shown in Figure 4. The absence of an observable optical rotation indicates that **2** is also racemic. Chiral HPLC separation gave (+)-**2** and (–)-**2** whose absolute configurations are identified as 1'S,6'S,7'S,10'S for (+)-**2** and 1'R,6'R,7'R,10'R for (–)-**2** by using computational methods (Supporting Information). It is interesting that the presence of the 1,4-dihydroxybenzene moiety in **2** makes it the first example of an meroterpenoid natural product with an intriguing 4/5/6/6/6 polycyclic ring system.

G. cochlear is regarded as one kind of Lingzhi for the treatment of various diseases.¹⁴ Our present findings in studies of meroterpenoids will aid our understanding of *Ganoderma* chemistry. To determine if racemic compounds **1** and **2** from

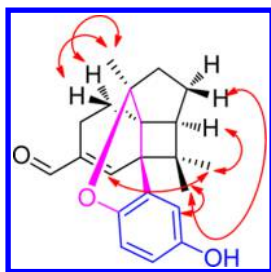


Figure 4. Key ROESY correlations of **2**.

G. cochlear exert renoprotective effects, a study with TGF- β 1-induced rat renal proximal tubular cells was conducted. The results showed that both racemic **1** and **2** inhibit upregulation of collagen I, fibronectin, and α -SMA in a dose-dependent manner, with **1** being more potent than **2** (Figure 5A,B). Since collagen I,

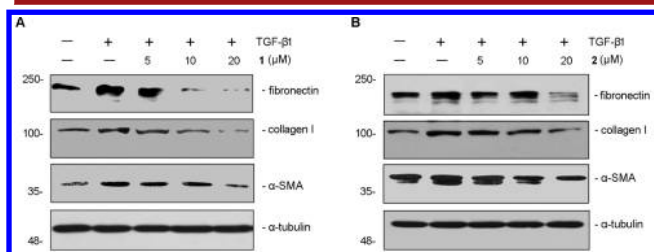


Figure 5. Compounds **1** and **2** inhibit fibrogenic action of TGF- β 1 in rat renal proximal tubular cells. NRK-cells were incubated with TGF- β 1 (5 ng/mL) for 48 h in the absence or presence of different concentrations (5–20 μ M) of compounds **1** (A) and **2** (B). Cell lysates after various treatments as indicated were immunoblotted with antibodies against fibronectin, collagen I, α -SMA, and α -tubulin.

fibronectin, and α -SMA production is a main hallmark of renal fibrosis, the finding suggests that **1** and **2** might have renoprotective effects, especially on renal fibrosis. Considering that the inhibition of collagen I, fibronectin, and α -SMA might be associated with the TGF- β /Smads signaling pathway, inhibition of Smad2/3 phosphorylation by racemic **1** and **2** was explored using Western blot. The results show that phosphorylation of Smad2 and Smad3 are indeed inhibited by **1** and **2** (Figures 6A and 6B), suggesting that both substances exert their antifibrotic actions by a mechanism dependent on disruption of Smad activation.

Because it is known that enantiomers of substances often have different biological activities, exemplified by those of *R*-/*S*-

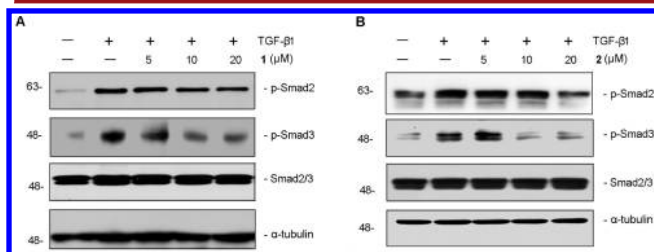


Figure 6. Compounds **1** and **2** selectively block TGF- β 1-mediated Smad2 and Smad3 phosphorylation in a dose-dependent manner. NRK-S2E cells were treated with TGF- β 1 (5 ng/mL) for 3 h in the absence or presence of different doses of **1** (A) or **2** (B) as indicated. Cell lysates after various treatments as indicated were immunoblotted with antibodies against phosphorylated Smad2, phosphorylated Smad3, total Smad2/3 and α -tubulin.

thalidomide, *R*-/*S*-warfarin, *R*-/*S*-chlorpheniramine, or *R*-/*S*-ketamine. To evaluate each the enantiomers of **1** and **2**, their renoprotective effects were evaluated in renal proximal tubular cells using PCR and Western blot. Surprisingly, two enantiomers of **1** show no apparent inhibitory effects as seen in the images in Figures 7 A and 7B, the PCR results of fibronectin, collagen I, and

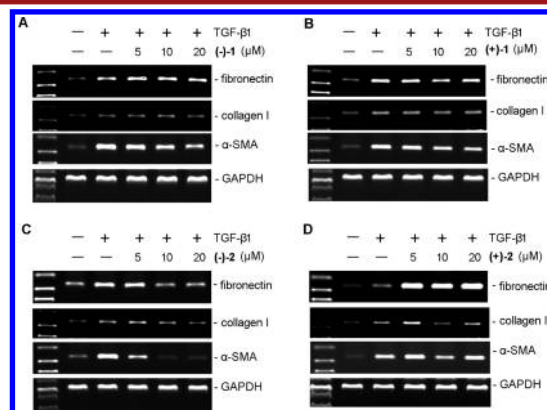


Figure 7. Enantiomers of **1** and **2** show different activities in inhibition of fibrogenic activation in rat renal proximal tubular cells. NRK-S2E cells were incubated with TGF- β 1 (5 ng/mL) for 48 h in the absence or presence of different concentrations (5 to 20 μ M) of (–)-antipodes (A or C) or (+)-antipodes (B or D). Total RNA was extracted and reverse transcribed RT-PCR were performed with different primers of fibronectin, collagen I, α -SMA, and GAPDH.

α -SMA. In addition, MTT assays demonstrate the toxic effects to cell viability of both enantiomers of **1** (Figure S15A, B, Supporting Information). However, (–)-**2** exerts its potent antifibrotic efficacy by a dose-dependent manner (Figure 7C), despite the fact that (+)-**2** is inactive (Figure 7D). Notably, two enantiomers of **2** show no effects to cell viability even with higher concentrations, as detected by MTT assay (Figure S15C, D, Supporting Information). To further assess the activity of enantiomers of **1** and **2**, we performed RT-PCR of fibrogenic genes, both enantiomers of compounds **1** and **2** alone could not significantly inhibit the fibrotic genes of fibronectin, collagen I and α -SMA (Figure S16, Supporting Information).

In addition, we determined if the (–)- and (+)-antipodes of **1** and **2** elicit antifibrotic effects by a mechanism involving disruption of Smad activation. Inspection of the images in Figure 8 shows that TGF- β 1 triggers a marked induction of phosphorylation of Smad2 and Smad3 in rat renal proximal tubular cells. Consistent with their antifibrotic efficacies, two enantiomers of **1** similarly display no apparent inhibitory effect on TGF- β 1 induced activation of p-Smad2 and p-Smad3 (Figure 8A, B). Clearly, more investigations are needed to assess the different activity of **1** and its enantiomers, as **1** shows evident inhibitory effects to TGF- β -induced fibrogenesis and Smad activation (Figures 5 and 6) when target protein was normalized to the structural protein, α -tubulin, despite of its bad effects to cell viability. However, (–)-**2** potentially disrupts Smad2 and Smad3 activation (Figure 8C) whereas (+)-**2** does not. Although more investigations are needed, our current studies provide proof that (–)-**2** can play potential roles in the therapy of renal fibrotic lesions by the disruption of Smad activation.

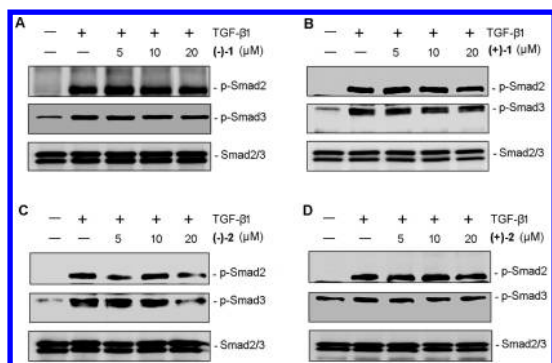


Figure 8. Enantiomers of **2**, but not **1**, block TGF- β 1-mediated Smad2 and Smad3 phosphorylation. NRK-52E cells were treated with TGF- β 1 (5 ng/mL) for 3 h in the absence or presence of different concentrations (5 to 20 μ M) of (–)-antipodes (A or C) or (+)-antipodes (B or D). Cell lysates after various treatments as indicated were immunoblotted with antibodies against phosphorylated Smad2, phosphorylated Smad3. Total Smad2/3 were used as normalizing control.

■ ASSOCIATED CONTENT

Supporting Information

1D, 2D NMR, and MS spectra, detailed isolation procedures, bioassay methods, computational methods, NMR data of **1** and **2**, and X-ray crystal data of (\pm)-**1**. This material is available free of charge via Internet at <http://pubs.acs.org>.

■ AUTHOR INFORMATION

Corresponding Authors

*(Y.X.C.) Phone/fax: +86-871-65223048. E-mail: yxcheng@mail.kib.ac.cn.

*(F.F.H.) E-mail: fffhouguangzhou@163.com.

*(R.T.L.) E-mail: lrt512@163.com.

Author Contributions

[#]These authors contributed equally.

Notes

The authors declare no competing financial interest.

■ ACKNOWLEDGMENTS

This study was supported by the NSFC-Joint Foundation of Yunnan Province (U1202222), a project from National Natural Science Foundation of China (21472199), and the Foundation for Distinguished Young Talents in Higher Education of Guangdong, China (C1031095) to L.L.Z.

■ REFERENCES

- (1) Ding, P.; Qiu, J. Y.; Liang, Y. J. *Chin. Tradit. Herb Drugs* **2010**, *2*, 65–67.
- (2) Yang, Z. L.; Feng, B. *Mycology* **2013**, *4*, 1–4.
- (3) Russel, R.; Paterson, M. *Phytochemistry* **2006**, *67*, 1985–2001.
- (4) Trigos, A.; Medellín, J. S. *Rev. Mex. Mic.* **2011**, *34*, 64–82.
- (5) Yan, Y. M.; Ai, J.; Zhou, L. L.; Arthur, C. K. C.; Li, R.; Nie, J.; Fang, P.; Wang, X. L.; Luo, J.; Hu, Q.; Hou, F. F.; Cheng, Y. X. *Org. Lett.* **2013**, *15*, 5488–5491.
- (6) Peng, X. R.; Liu, J. Q.; Xia, J. J.; Yang, X. *Chin. Tradit. Herb Drugs* **2012**, *43*, 1045–1049.
- (7) Peng, X. R.; Liu, J. Q.; Wang, C. F.; Yang, X.; Qiu, M. H. *J. Nat. Prod.* **2014**, *77*, 737–743.
- (8) Peng, X. R.; Liu, J. Q.; Wan, L. S.; Li, X. N.; Yan, Y. X.; Qiu, M. H. *Org. Lett.* **2014**, *16*, 4838–4841.
- (9) Peng, X. R.; Liu, J. Q.; Wang, C. F.; Han, Z. H.; Shu, Y.; Li, X. Y.; Zhou, L.; Qiu, M. H. *Food Chem.* **2015**, *171*, 251–257.

(10) Cochlearol A (**1**): yellow crystalline solid; $[\alpha]_D^{24}$ 0 (c 0.12, MeOH); UV (MeOH) λ_{max} (log ϵ) 369 (3.62), 203 (4.15) nm; ^1H and ^{13}C NMR data, see Table S1 (Supporting Information); ESIMS (negative) m/z 306 $[\text{M} - \text{H}]^-$; HREIMS m/z 306.0752 $[\text{M}]^+$ (calcd for $\text{C}_{15}\text{H}_{14}\text{O}_7$ 306.0740); $[\alpha]_D^{25}$ –48.3 (c 0.18, MeOH); CD (MeOH) $\Delta\epsilon_{200}$ –33.9, $\Delta\epsilon_{213}$ –22.32, $\Delta\epsilon_{239}$ –11.77, $\Delta\epsilon_{273}$ –5.25; (–)-cochlearol A; $[\alpha]_D^{25}$ +50.0 (c 0.18, MeOH); CD (MeOH) $\Delta\epsilon_{200}$ +19.66, $\Delta\epsilon_{213}$ +37.45, $\Delta\epsilon_{239}$ +18.64, $\Delta\epsilon_{273}$ +4.90; (+)-cochlearol A.

(11) Crystallographic data of cochlearol A (**1**) have been deposited at the Cambridge Crystallographic Data Centre (deposition no. CCDC 1012020). Copies of the data can be obtained free of charge via www.ccdc.cam.ac.uk/conts/retrieving.html.

(12) Cochlearol B (**2**): yellow amorphous solid; $[\alpha]_D^{25}$ 0 (c 0.12, MeOH); UV (MeOH) λ_{max} (log ϵ) 296 (3.62), 228 (4.25), 203 (4.34) nm; ^1H and ^{13}C NMR data, see Table S1 (Supporting Information); ESIMS (negative) m/z 324 $[\text{M} - \text{H}]^-$; HREIMS m/z 324.1710 $[\text{M}]^+$ (calcd for $\text{C}_{21}\text{H}_{24}\text{O}_3$ 324.1725); $[\alpha]_D^{25}$ –160.2 (c 0.19, MeOH); CD (MeOH) $\Delta\epsilon_{205}$ +148.19, $\Delta\epsilon_{227}$ –192.99, $\Delta\epsilon_{246}$ –136.59, $\Delta\epsilon_{332}$ +9.20; (–)-cochlearol B; $[\alpha]_D^{25}$ +154.6 (c 0.17, MeOH); CD (MeOH) $\Delta\epsilon_{205}$ –138.20, $\Delta\epsilon_{227}$ +183.62, $\Delta\epsilon_{246}$ +130.45, $\Delta\epsilon_{332}$ –12.17; (+)-cochlearol B.

(13) Weyerstahl, P.; Marschall, H.; Christiansen, C.; Seelmann, I. *Liebigs Ann.* **1996**, 1996, 1641–1644.

(14) (a) Reishi, K. J. *Ancient Herbs for Modern Times*; Sylvan Press: London, 1992. (b) Lin, Z. B., Ed. *Modern Research on Lingzhi*, 2nd ed.; Beijing Medical University Press: Beijing, 2001.